35th Annual International Conference of the IEEE EMBS
Osaka, Japan, 3 - 7 July, 2013

Computer-Aided Liver Surgical Planning System Using CT Volumes

Yen-Wei Chen, *IEEE Member,* Masaki Kaibori, Tsukasa Shindo, Kousuke Miyawaki, Tsukasa Shindo, Amir H. Foruzan, Tomoko Tateyama, Xian-Hua Han, Kosuke Matsui, Takumi Tsuda, A-Hon Kwon

***Abstract*—In this paper, we presented our newly developed computer-aided liver surgical planning system for patient-specific treatments by using the patient's CT volumes. The system is composed of three modules, liver segmentation, vessel extraction, and visualization & interaction modules. It can prepare a virtual environment for patient-specific liver surgical planning and simulations. We also developed an original visualization library, which is based on GPU (graphics processing unit) computing for real-time interaction and visualization. The effectiveness of our system was evaluated by surgeons with liver surgery simulations.**

I. Introduction

It is important to know the liver geometry, its vessels structures, liver's tumors sizes and locations in pre-surgical planning. Recently, an increasing interest has been seen in virtual surgical planning and simulation systems [1-7]. The virtual surgical planning system is an integration of medical image analysis, computer graphics and virtual reality techniques. The system can prepare a virtual environment for surgeons to perform surgical planning and simulations. In our previous works, we developed a patient-specific computer aided liver surgical planning system [8-10]. In our previous system (1st generation), we used the Visualizing Tool Kit (VTK) library [11] for visualization and interaction as well as almost existing surgical planning system. However, VTK is only used for CPU processing and its processing time is long, making it unsuitable for a real-time interactive surgical simulation system. To accelerate the speed of visualization and interaction, we have developed an original visualization library [12] based on GPU (graphics processing unit) computing.

In this paper, we present our newly developed computer aided liver surgical planning and simulation system (2nd generation). The main improvements are shown in below:

(1) The system is developed based on our original GPU based visualization library [11], which makes real-time interactive surgical simulation possible even with high-resolution CT volumes.

(2) The surgeon's prior knowledge and clinical experience were integrated into the visualization system to create a practical virtual surgery, leading to improved functionality and accuracy of information recognition in the surgical simulation system.

(3) The effectiveness of our system was evaluated by surgeons with liver surgical simulations.

This paper is organized as follows. In Sec.2 we describe our liver surgical planning system. Surgical simulation results are presented in Sec. 3. The conclusion and future work are given in Sec.4.

II. Surgical Planning System

Our system is composed of three main modules: Liver segmentation module, vessel extraction module, and visualization & interaction module as shown in Fig.1.

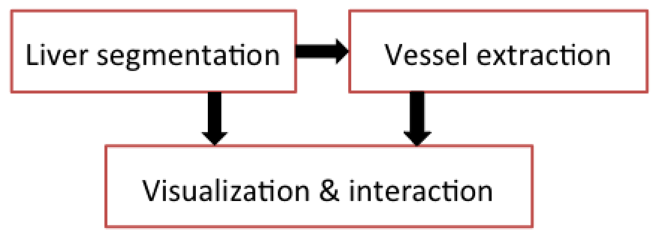

Figure 1. Three modules of our liver surgery planning system

A. Liver Segmentation Module

Liver segmentation module finds the surface of the liver in CT datasets of different phases. In this module, we use a robust liver segmentation method, which was developed in our previous works [13].

The process of our proposed liver segmentation method is shown in Fig.2. The typical slice of CT images is shown in Fig.2(a). Liver segmentation starts with preprocessing which includes elimination of noise, defining the body's Volume Of Interest to reduce the size of image and increase the speed of the code, removing some non-liver tissues, and manual segmentation of liver in a large slice. We use the fact that liver is inside ribs to remove muscles that are both between and behind ribs. The intensity range of these muscles has intersections with that of liver, so they are removed in preprocessing step. Please see Ref.13 for details about the preprocessing. Starting from the mask of liver in manually segmented slice whose histogram is shown in Fig.2(b), we assume a Gaussian mixture model with two components ($G(\mu_i, \sigma_i \mid \pi_i), 1 \le i \le 2$) to model intensity distribution of liver and tumors. We employ EM to find statistical parameters of mixture model as shown in Fig.2(c).

For each mode i of the mixture model, we threshold new slices in the region [$\mu_i - \beta\sigma_i, \mu_i + \beta\sigma_i$] (Narrow band thresholding) to find liver candidate pixels, where $\beta = 0.75$. The narrow band thresholding results (liver candidate pixels)

*Resrach supported by the Grant-in Aid for Scientific Research from the Japanese MEXT (No. 2430076, No,24103710, No.24700179) and R-GIRO.

Y. W. Chen is with the Central South Univ. of Forestry and Technology, Hunan, China and the Ritsumeikan University, Shiga, Japan (phone: +81-77-545-5078; fax: +81-303-555-5555; e-mail: chen@is.ritsumei.ac.jp).

K. Miyawaki, T. Shindo, T. Tateyama and X. Han are with the College of Information Science and Engineering, Ritsumeikan Univ., Shiga, Japan

A. H. Foruzan is with the Department of Biomedical Engineering, Engineering Faculty, Shahed University, Tehran, Iran.

M. Kaibori, K. Matsui, T. Tsuda and A. Kwon are with the Department of Surgery, Kansai Medical University, Osaka, Japan.

is shown in Fig.2(d). K-means is employed to reject non-liver pixels and remain liver's index pixels (cluster centers) as shown in Fig.2(e) (yellow circles). Then, the original image is thresholded in the whole range of each mode i ($[\mu_i - 3\sigma_i, \mu_i + 3\sigma_i]$), so that more pixels are involved. We assign to the new pixels a probability $p(x) = 1/d(x)$; where $d(x)$ is the Hausdorff distance of a pixel to index pixels. In this way, we establish liver probability map as shown in Fig.2(f). We threshold the map to find the boundary of liver and smooth it using Fourier transform (Fig.2(g)), which is used as an initial boundary of the liver. As the final step of the liver segmentation algorithm, the initial liver surface (Fig.2(g)) is used as the input to a 3D geodesic active contour [14]. A few iteration of the active contour algorithm is needed to find the final result as shown in Fig.(h).

B. Vessel Extraction Module

Vessel information is very important for surgery simulation, which is also a key factor for being considered by doctor in surgery procedure. Therefore, we want to render the accurate positions of different types vessels in our surgery simulation system. Then, the vessel extraction is also a necessary pre-procedure. In this research, we extract the line-like structure (vessel structure) using Hessian matrix proposed by Frangi.[15] Eigen vectors of the Hessen matrix for each pixel can represent orientation of shape at some scale. For Vessel structure, the corresponding Eigenvector of the smallest eigenvalue shows running direction of vessel, and the corresponding eigenvector of the largest eigenvalue

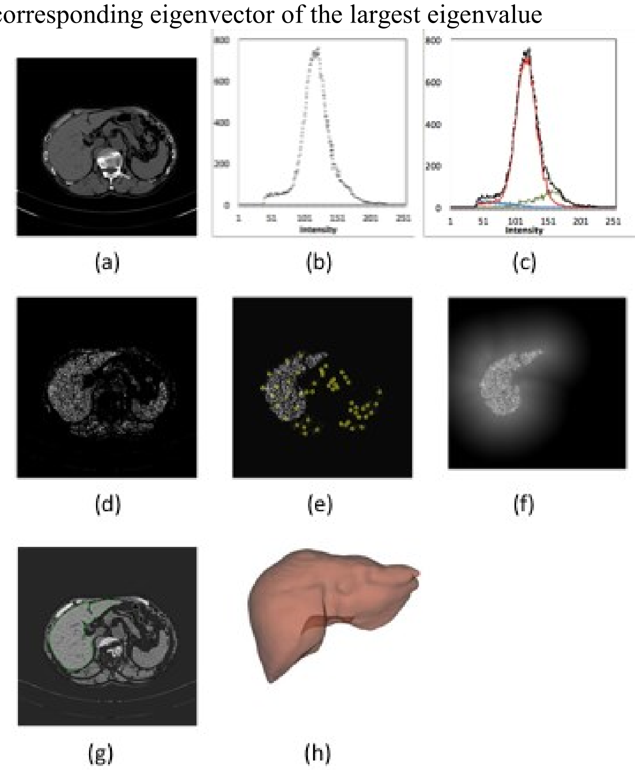

Figure 2. The process of our proposed liver segmentation method [13]. (a) Original image, (b) histogram of the liver region, (c) two components obtained by EM, (d) candidate liver pixels by narrow band thresholding, (e) clustered pixels to find liver index pixels (Cluster centers are shown as yellow circles), (f) probability map based on liver index pixels, (g) segmented liver, (h) iso-surface view of the final segmented liver.

shows vertical direction of running one. Given the eigenvalues λ_1, λ_2, λ_3 with $|\lambda_1| \leqq |\lambda_2| \leqq |\lambda_3|$, the correspondence between shape structure and eigenvalues are summarized in Table 1.

For implementation, the normalized Gaussian filter is used for improving the contrast between vessels and background. Since it is difficult to enhance vessels with different size by one scale Gaussian filter, a multi-scale filter, which can adjust the filter width according to pixel intensity information, is used for enhancing vessel structure with different sizes [15].

In our vessel extraction module, the segmented livers are used as masks for vessel extraction. Hepatic artery, portal vein, and hepatic vein are extracted from the arterial phase (the first phase), the portal-venous phase (the second phase), and the delayed phase (the third phase) of CT images, respectively. The roots of these vessels are usually outside of the liver mask. We add the roots of the vessels to the vascular structures and trimming the results. The extracted hepatic artery, portal vein, and hepatic vein are shown in Fig.3(a), 3(b) and 3(c), respectively.

In order to visualize these three vessels with segmented liver model together, we employed the surface of liver from the second phase as the liver model and register segmented livers of the first and third phases to the model before vessel extraction. Registration is performed using "Iterative Closest Point" algorithm [16] and the resultant transform matrices are used to register portal artery and hepatic vein [9]. The visualized liver and its vessel structure is shown in Fig.3(d).

Table 1 Eigen values ($|\lambda_1| \leqq |\lambda_2| \leqq |\lambda_3|$) vs. pattern
(N: Noisy L: Low value H: High value +/-: sign)

λ_1	λ_2	λ_3	pattern
N	N	N	noisy, no preferred direction
L	L	H-	Bright plate structure
L	L	H+	Dark plate structure
L	H-	H-	Bright tubular structure
L	H+	H-	Dark tubular structure
H-	H-	H-	Bright Blob structure
H+	H+	H+	Dark Blob structure

C. Visualization and Interaction Module

In our new system (2^{nd} generation), we use our original GPU based visualization library [11] for visualization and interactions instead of the conventional VTK. It makes real-time interactive surgical simulation possible even with high-resolution CT volumes.

The visualization and interaction module is shown in Fig.4. In a surgical simulation system, the input device is expected to replicate the movements of a real scalpel. Since it was impossible to control the input position of the virtual blade accurately using conventional input devices such as a keyboard and mouse, we use a pen-like haptic 3D pointing device (Phantom Omni haptic device) [17] to simulate a real scalpel in our system. The Omni haptic pointing device's high fidelity force feedback senses motion in 6 degrees of freedom to make it possible to touch and manipulate virtual

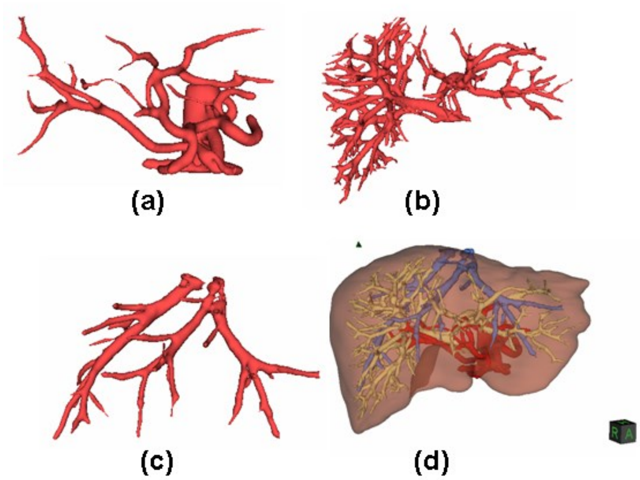

Figure 3. (a) Hepatic artery, (b) portal vein, (c) hepatic vein, (d) liver and its vascular structure. In (d), hepatic artery, portal vein, and hepatic vein are colored in red, yellow, and blue, respectively.

objects in all axes [17]. The position of its tip reflects the cutting point in virtual space. The coordinate of the cutting point (3D pointing device coordinate system) is then converted into the viewing coordinate system.

Five volume data (the segmented liver, the extracted hepatic artery, portal vein, hepatic vein, and manually segmented tumor) are used in our surgical systems. They are registered and visualized together as shown in Figs.6 and 7. We cut the volumes based on the cutting information (position and region) inputted by the 3D pointing device. The cutting region (or the deformation) was determined by the pressure applied to the 3D pointing device. We then rebuild the surface of the cut volume by using a marching cube algorithm [18]. In order to accelerate the computation time, the volume is divided into several small volumes with a size of $32 \times 32 \times 32$. We calculate only about the small deformation domain. The cutting (or deformation), the marching cube algorithm and surface rendering are performed on GPU with our original visualization library. Compared with our previous system (1st generation), our new system (2nd generation) makes a real-time interactive simulation possible even with high-resolution CT volumes. The comparison of surface generation time (the marching cube algorithm) between our new system and the previous system [8-10] is shown in Table 2. Finally, our new system can display the deformation by resections at the high speed of 20~40 FPS.

Table 2 The comparison of surface generation time between our proposed system and the previous system [8-10]

Volume Size	New system	Previous system
$32 \times 32 \times 32$	120FPS	40FPS
$128 \times 128 \times 128$	0.5~3FPS	0.3~0.5FPS

D. Our System

Our surgical simulation system is developed on a computer with the specifications as follows; graphic board (GeForce 8700M GT, 1.52GB), CPU (Intel i7-2600, 3.40GHz~3.9GHz), GPU (nVidia Quadro 4000), Memory (8.00GB), and 3D display (Samsung, SyncMaster2233RZ). The 3D display has a refresh rate of 120 Hz.

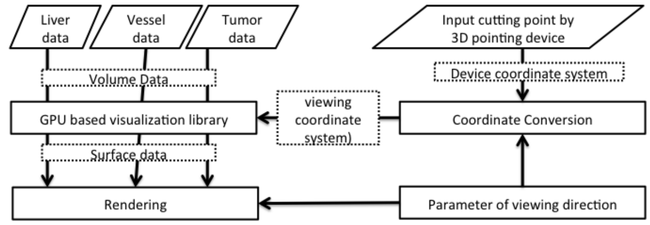

Figure 4. The visualization and interaction module

The system is shown in Fig.5. Based on the surgeon's prior knowledge and clinical experience, our system consists of four screens. The right two windows are main screens reflecting the relative position between the virtual knife and the liver model. The upper right image is an opaque liver, while the lower right window is its transparent version with the visible vessel structure. The left two windows are assistance screens to show the locally visible liver and vessels (in detail) or the global vessels from different angles.

III. SIMULATION RESULTS

Surgical simulations have been done by a surgeon with our system as shown in Fig.5. Two typical examples are shown in Fig.6 and Fig.7. The first simulation (Fig.6) is to resect the S8 subsegment in order to remove a small liver tumor located in the right lobe upper part (green one in Fig.6(a). The second simulation (Fig.7) is to resect the hepatic right trisegmentectomy in order to remove a large tumor in right lobe which is shown with dark gray in Fig.7(a). Both tumors are segmented from the CT image manually. Fig.6(a) and 7(a) show screens before the surgical operation and Fig.6(b) and 7(b) are results after the operation. We can see that the tumor was perfectly resected in both cases. S.

After using our system, two surgeons completed a subjective satisfaction questionnaire as shown in Table 3. It can be seen that visualization and operation are satisfying, but the reality of the surgical simulation still needs to improve for practical use.

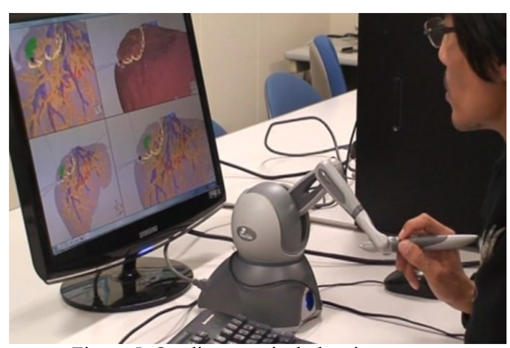

Figure 5. Our liver surgical planning system

Table 3. The quantitative results of the user study questionnaire

	Visualization	Operation	Reality	Practical
Surgeon1	Good	Easy	Good	Yes
Surgeon2	Good	Easy	Not good	No

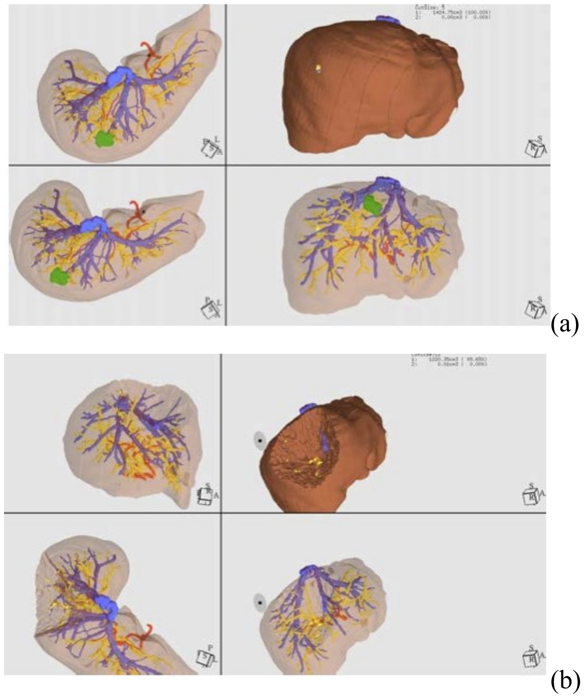

Figure 6. Surgical simulation1: resection of the S8 subsegment including a small liver tumor. (a) before resection, (b) after resection

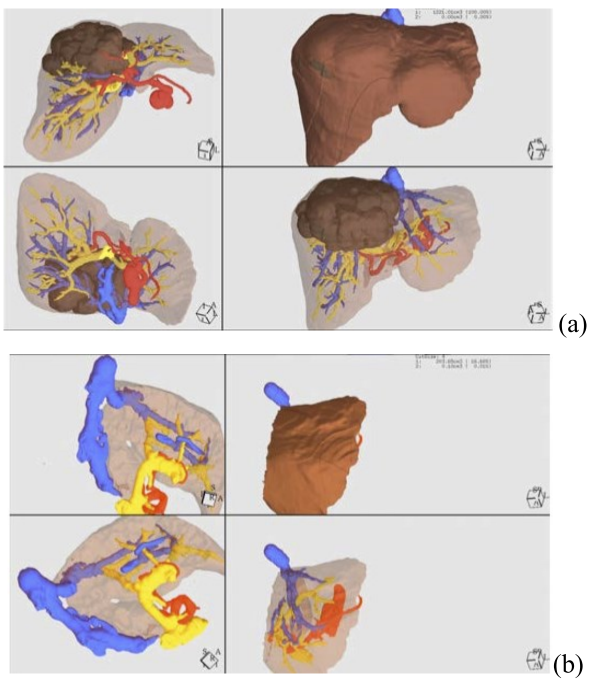

Figure 7. Surgical simulation2: resection of the hepatic right trisegmentectomy. (a) before resection, (b) after resection

IV. CONCLUSION

In this paper, we constructed a new liver surgery planning and simulation system (2nd generation) for individual patient, with his/her CT volume. We also developed a GPU based original visualization library for real time visualization and interactions. The system can display the deformation by resections at the high speed of 20~40 FPS. The simulation system can reproduce the real surgery procedure for guiding doctors' operation. In addition, it is implemented according to doctors' experience and prior knowledge for specific individual patient, interactive operation and 3D visualization. Therefore, it can be used not only for assisting surgery planning but also doctors' training and education, prior explanation for real surgery..

REFERENCES

[1] H.P. Meinzer, et. al. "Computer- based Surgery Planning for Living Liver Donation," *20th ISPRS Congress, Istanbul 2004,* pp.291-295.

[2] J.S. Fong and H. Ibrahim, "Development of a virtual reality system for Hepatocellular Carcinoma pre-surgical planning," *2nd International Conference on Software Technology and Eng.*, 2010, pp. 41-45.

[3] X. Song et. al., "Computer-aided Preoperative Planning for liver Surgery based on CT Images", *Procedia Engineering,* Vol.24, 2011, pp. 133-137.

[4] D. Selle, et al., "Analysis of Vasculature for Liver Surgical Planning", *IEEE Trans. Med. Imag*., 2002, pp.1344-1357.

[5] N. Shevchenko, et al., "MiMed liver: A planning system for liver surgery Engineering", in *Medicine and Biology Society (EMBC), 2010 Annual International Conference of the IEEE*, 2010, pp.1882-1885.

[6] B. Reitinger at al., "Liver Surgery Planning Using Virtual Reality," *IEEE Computer Graphics and Applications*, November/December, 2006, pp.36-47.

[7] B. Reitinger, Virtual Liver Surgery Planning: Simulation of Resections Using Virtual Reality Techniques, *Ph.D Dissertation, Graz Univ. of Technology*, 2005.

[8] T. Shindo, Y,-W Chen, M. Kaibori, et al., "3D Visualization of Liver and Its Vascular Structures and Surgical Planning System," *in ICCIT2011*, Jeju, Korea, 2011, pp.939-944.

[9] A.H. Foruzan, Y.-W. Chen, M.Kaibori et al., "Analysis of CT Images of Liver for Surgical Planning," *Am. J. of Biomedical Eng*. 2, 2012, pp. 23-28.

[10] T. Tomoko, M.Kaibori, Y.-W.Chen et al., "Patient-Specified 3D Visualization of Liver and Vascular Structures and Interactive Surgical Planning System," *Medical Imaging Technology,* Vol.31, No.3, 2013, in press. (in Japanese)

[11] Visualization toolkit, http://www.vtk.org/

[12] K. Miyawaki, *Graduation Thesis of Ritsumeikan University*, 2011.

[13] A. H. Foruzan, Y.-W. Chen at. al., "Segmentation of Liver in Low-contrast Images Using K-Means Clustering and Geodesic Active Contour Algorithms," *IEICE Trans*., Vol.E96-D, 2013, pp.798-807.

[14] V. Caselles, et. al., "Geodesic active contours," *International Journal on Computer Vision*, vol. 22, no. 1, 1997, pp. 61–97.

[15] A.F. Frangi, et. al., "Multiscale vessel enhancement filtering," *In Proc. 1st MICCAI,* 1998, pp. 130-137..

[16] Z. Zhang, "Iterative point matching for registration of free-form curves," *Research Report 1658, INRIA So- phia-Antipolis*, 1992.

[17] Phantom Omni Haptic Device: http://www.sensable.com/haptic-phantom-omni.htm

[18] W.E. Lorensen and H.E. Cline, "Marching cubes: A high resolution 3D surface construction algorithm", *Computer Graphics (Proceedings of SIGGRAPH'87)*, Vol.21, No.4, 1987, pp.163-170.